Cellular/Molecular

Autism Spectrum Disorder/Intellectual Disability-Associated Mutations in Trio Disrupt Neuroligin 1-Mediated Synaptogenesis

Chen Tian,[1,2*] Jeremiah D. Paskus,[3*] Erin Fingleton,[3] Katherine W. Roche,[3] and Bruce E. Herring[1]

[1]Section of Neurobiology, Department of Biological Sciences, University of Southern California, Los Angeles, California 90089, [2]Neuroscience Graduate Program, University of Southern California, Los Angeles, California 90089, and [3]Receptor Biology Section, National Institute of Neurological Disorders and Stroke, National Institutes of Health, Bethesda, Maryland 20892

We recently identified an autism spectrum disorder/intellectual disability (ASD/ID)-related *de novo* mutation hotspot in the Rac1-activating GEF1 domain of the protein Trio. Trio is a Rho guanine nucleotide exchange factor (RhoGEF) that is essential for glutamatergic synapse function. An ASD/ID-related mutation identified in Trio's GEF1 domain, Trio D1368V, produces a pathologic increase in glutamatergic synaptogenesis, suggesting that Trio is coupled to synaptic regulatory mechanisms that govern glutamatergic synapse formation. However, the molecular mechanisms by which Trio regulates glutamatergic synapses are largely unexplored. Here, using biochemical methods, we identify an interaction between Trio and the synaptogenic protein Neuroligin 1 (NLGN1) in the brain. Molecular biological approaches were then combined with super-resolution dendritic spine imaging and whole-cell voltage-clamp electrophysiology in hippocampal slices from male and female rats to examine the impact ASD/ID-related Trio mutations have on NLGN1-mediated synaptogenesis. We find that an ASD/ID-related mutation in Trio's eighth spectrin repeat region, Trio N1080I, inhibits Trio's interaction with NLGN1 and prevents Trio D1368V-mediated synaptogenesis. Inhibiting Trio's interaction with NLGN1 via Trio N1080I blocked NLGN1-mediated synaptogenesis and increases in synaptic NMDA Receptor function but not NLGN1-mediated increases in synaptic AMPA Receptor function. Finally, we show that the aberrant synaptogenesis produced by Trio D1368V is dependent on NLGN signaling. Our findings demonstrate that ASD/ID-related mutations in Trio are able to pathologically increase as well as decrease NLGN-mediated effects on glutamatergic neurotransmission, and point to an NLGN1-Trio interaction as part of a key pathway involved in ASD/ID etiology.

Key words: AMPA Receptor; dendritic spine; glutamatergic synapse; neurodevelopmental disorder; NMDA Receptor; RhoGEF

Significance Statement

A number of genes have been implicated in the development of autism spectrum disorder/intellectual disability (ASD/ID) in humans. It is now important to identify relationships between these genes to uncover specific cellular regulatory pathways that contribute to these disorders. In this study, we discover that two glutamatergic synapse regulatory proteins implicated in ASD/ID, Trio and Neuroligin 1, interact with one another to promote glutamatergic synaptogenesis. We also identify ASD/ID-related mutations in Trio that either inhibit or augment Neuroligin 1-mediated glutamatergic synapse formation. Together, our results identify a synaptic regulatory pathway that, when disrupted, likely contributes to the development of ASD/ID. Going forward, it will be important to determine whether this pathway represents a point of convergence of other proteins implicated in ASD/ID.

Received Mar. 2, 2021; revised July 19, 2021; accepted July 24, 2021.

Author contributions: C.T., J.D.P., and B.E.H. designed research; C.T. performed electrophysiology and imaging experiments; J.D.P. and E.F. performed biochemical experiments; C.T., J.D.P., and E.F. analyzed data; C.T., J.D.P., E.F., K.W.R., and B.E.H. wrote and edited the paper.

This work was supported by the Brain and Behavior Research Foundation to B.E.H., the Simons Foundation to B.E.H., the McKnight Foundation to B.E.H., National Institute of Mental Health R00MH103398 to B.E.H., and National Institute of Neurological Disorders and Stroke R01NS112480 to B.E.H. Funds supporting this work were also provided by a University of Southern California Theodore and Wen-Hui Chen Endowed Fellowship to C.T., and the National Institute of Neurological Disorders and Stroke Intramural Research Program to J.D.P., E.F., and K.W.R. We thank members of B.E.H. and K.W.R. laboratories for helpful feedback during the study.

*C.T. and J.D.P. contributed equally to this work as co-first authors.

The authors declare no competing financial interests.

Correspondence should be addressed to Bruce E. Herring at bherring@usc.edu.

https://doi.org/10.1523/JNEUROSCI.3148-20.2021

Introduction

Increasing evidence suggests that autism spectrum disorder (ASD) pathogenesis can be attributed to excitatory synapse dysfunction (Bourgeron, 2015; Volk et al., 2015; Martinez-Cerdeno, 2017). Glutamatergic synapses, the primary excitatory synapses in the brain, are formed on mushroom-like protrusions called dendritic spines. These spines are filled with and supported by a dense skeletal meshwork of actin filaments. Exome sequencing studies reveal that many ASD risk factors influence dendritic spine structure and function (De Rubeis et al., 2014; Forrest et al., 2018; Joensuu et al., 2018). The small GTPase Rac1, a key regulator of actin polymerization in dendritic spines, has also been

proposed as a promising candidate of convergence of many ASD risk factors (Schenck et al., 2003; Dolan et al., 2013; Zeidán-Chuliá et al., 2013; Duffney et al., 2015; Tian et al., 2018; Guo et al., 2021).

The Rho guanine nucleotide exchange factor (RhoGEF) Trio and its paralog, Kalirin, play an essential role in glutamatergic synapse structure and function through their ability to activate Rac1 (Bellanger et al., 2000; Penzes et al., 2001; Penzes and Jones, 2008; Penzes and Remmers, 2012; Herring and Nicoll, 2016; Katrancha et al., 2019; Paskus et al., 2020). We recently identified a cluster of disruptive ASD/ID-related *de novo* mutations in the Rac1-activating domain of Trio, GEF1 (Sadybekov et al., 2017). One missense mutation, Trio D1368V, increases Trio's ability to activate Rac1 and results in a pathologic increase in glutamatergic synaptogenesis. The molecular mechanisms by which Trio D1368V facilitates synaptogenesis are unresolved. Understanding how ASD/intellectual disability (ID)-related mutations give rise to elevated synaptogenesis is of great interest given that pathologic elevations in glutamatergic synapse formation have been observed in a number of animal models of ASD/ID as well as in many individuals with ASD/ID (Comery et al., 1997; Irwin et al., 2001; Hutsler and Zhang, 2010; Tang et al., 2014).

To identify ASD/ID-related Trio protein interactions that are involved in synaptogenesis, we investigated the ASD/ID-related mutation Trio N1080I within Trio's eighth spectrin repeat. Spectrin repeats support protein interactions that govern a protein's participation in cellular regulatory pathways (Djinovic-Carugo et al., 2002). Here, we found that the aberrant synaptogenesis produced by the Trio D1368V mutation was abolished by adding the N1080I mutation to our Trio D1368V expression construct. This finding led us to ask whether Trio N1080 supports Trio's ability to interact with synaptogenic proteins. We have shown previously that both Trio and Kalirin bind to the highly synaptogenic protein Neuroligin 1 (NLGN1) in the brain (Bemben et al., 2015; Paskus et al., 2019). While Kalirin was found to bind to NLGN1 more strongly than Trio, an interaction between Trio and NLGN1 was detectable (Paskus et al., 2019). NLGN1 is a member of the NLGN protein family. NLGNs are well-established postsynaptic cell-adhesion molecules that share considerable similarity in protein domain structure. Through their interaction with presynaptic neurexins, NLGN proteins play essential and overlapping roles in glutamatergic synaptogenesis (Bemben et al., 2015). In the present study, we confirm that Trio binds to NLGN1 in the brain and supports NLGN1 function. This relationship between Trio and NLGN1 is of particular interest given that both Trio and NLGN1 are implicated in ASD/ID-related disorders (Blundell et al., 2010; Nakanishi et al., 2017; Sadybekov et al., 2017; Barbosa et al., 2020). Here, we discover that Trio N1080I inhibits Trio's ability to bind to NLGN1, and that Trio N1080I expression inhibits NLGN1-mediated synaptogenesis and NLGN1's influence on synaptic NMDA Receptor (NMDAR) function but not synaptic AMPA Receptor (AMPAR) function. Together, these findings led us to ask whether Trio D1368V's ability to increase synaptogenesis is supported by NLGN1. As predicted, we find that inhibition of NLGN signaling in neurons prevents Trio D1368V from generating new synapses. Thus, elevated Rac1 activation produced by the D1368V mutation serves to boost NLGN-mediated glutamatergic synapse formation. Together, our findings demonstrate that that ASD/ID-related mutations in Trio are able to increase as well as decrease NLGN-mediated synaptogenesis, and point to an NLGN1-Trio interaction as part of a key pathway involved in ASD/ID-related disorders.

Materials and Methods

Electrophysiology. Organotypic hippocampal slice cultures (400 μm) were prepared from P6-P8 Sprague Dawley male and female rat pups as described previously (Stoppini et al., 1991). Culture media was exchanged every other day. Sparse biolistic transfections of organotypic slice cultures were conducted on DIV1 as previously described (Schnell et al., 2002). Construct expression was confirmed by GFP and mCherry cotransfection. Paired whole-cell recordings from transfected neurons and nontransfected control neurons were performed on DIV7 slices. This study was conducted in accordance with the National Institutes of Health's *Guide for the care and use of laboratory animals*, and the protocol was approved by the University of Southern California Institutional Animal Care and Use Committee.

Coefficient of variation (CV) analysis. CV analysis was performed on AMPAR-eEPSCs by comparing the change in eEPSC variance with the change in mean amplitude as previously described (Bekkers and Stevens, 1990; Malinow and Tsien, 1990; Gray et al., 2011; Tian et al., 2018; Rao et al., 2019). Briefly, the mean and SD of eEPSCs were measured, normalized, and plotted for a concurrent set of stimuli from a control and its neighboring transfected cell. It has been shown theoretically and experimentally that changes in CV^{-2} ($mean^2/SD^2$) are independent of quantal size but vary in a predictable manner with quantal content: number of release sites $n \times$ presynaptic release probability, Pr; $CV^{-2} = nPr/(1 - Pr)$ (Del Castillo and Katz, 1954; Bekkers and Stevens, 1990; Xiang et al., 1994). CV analysis is presented here as scatterplots with CV^{-2} values calculated for transfected cell/control cell pairs on the y axis and mean eEPSC amplitude values of transfected cell/control cell pairs on the x axis. Filled circles represent the mean ± SEM of the entire dataset. Simple linear regression was obtained using the least-squares method. Regression lines that fall on or near the 45° ($y = x$) line suggests changes in quantal content, whereas regression lines approaching the horizontal line ($y = 1$) suggests a change in quantal size. Unsilencing of synapses can mimic an increase in the number of release sites when presynaptic release probability is unchanged.

Spine density analysis. For spine density analysis, control and experimental CA1 pyramidal neurons in organotypic hippocampal slice cultures made from P6-P8 rat pups were biolistically transfected with FUGW-GFP and pCAGGS-IRES-mCherry constructs ~18-20 h after plating (Kay and Herring, 2021). Images were acquired at DIV7 using super-resolution microscopy (Elyra Microscope System, Carl Zeiss). *Z* stacks were made of 30 μm sections of secondary apical dendrites ~30 μm from the soma. Images were acquired with a 100× oil objective (100×/1.46) in SIM mode using a supplied 42 μm SIM grating and processed and reconstructed using supplied software (Zen, Carl Zeiss). An experimenter, blinded to the condition of the image, performed image analysis on individual sections using ImageJ to count spines extending laterally from the dendrite.

Immunoblotting and immunoprecipitation. For coimmunoprecipitation experiments of endogenous protein, Sprague Dawley outbred adult rat brains (>3 months of age) were homogenized and fractionated as described previously (Paskus et al., 2019). Brains were homogenized in ice-cold TEVP buffer containing 320 mM sucrose with protease and phosphatase inhibitors. Samples were centrifuged and supernatants were centrifuged once more to collect crude synaptosomes (P2). P2 pellets were solubilized for 30 min at 37°C. The resultant solution was incubated on ice for 30 min and centrifuged again for 20 min. The supernatant was used for immunoprecipitation of endogenous proteins. For immunoprecipitation of proteins expressed in heterologous cells, HEK293T cells were maintained and processed as described previously (Paskus et al., 2019). Briefly HEK293T cells were transfected using Lipofectamine 2000. Forty-eight hours following transfection, cells were washed and lysed. Lysates were rocked for 1 h and centrifuged. Supernatants were collected and used for immunoprecipitation with HA beads incubated overnight at 4°C. Blots were quantified using Fiji.

Rac1 and RhoA activity assays. Rac1 activity was assessed using the Thermo Scientific Active Rac1 Pull-Down and Detection Kit (catalog #16118) according to the manufacturer's instructions. Briefly, HEK293T

cells were transfected with 5 μg of either WT Trio-9 or N1080I Trio-9. After 18-24 h, HEK293T cells were lysed and subjected to Rac1 pulldown and run on 12% SDS-PAGE, for Rac1 blotting, or 6% SDS-PAGE, for Trio-9 blotting, at 60-100 V for 1.5 h, then transferred in 10% methanol buffer at 350 mA for 1.5 h. Blots were probed with manufacturer-provided Rac1 antibody or Trio antibody (Paskus et al., 2019) at 4°C overnight, then incubated with HRP-conjugated secondary antibody at room temperature for 1 h. Western blot images were collected on the Bio-Rad ChemiDOC imaging system. RhoA activity was assessed using the Cell Signaling Technology Active Rho Detection kit (catalog #8820S) according to the manufacturer's instructions. Sample preparation and Western blotting were accomplished as in the Rac1 activity assay.

Experimental design and statistical analyses. Data were analyzed using a combination of in-house software in Igor Pro (WaveMetrics), ImageJ, Microsoft Excel, and R. For electrophysiological data, Wilcoxon Signed Rank Test was used for pairwise comparisons and Wilcoxon Rank Sum Test was used to compare across independent conditions. For CV analysis, linear regression analysis was performed using the least-squares method with R. Imaging analysis was performed blind to genotype. At least 2 male and 2 female rat pups were used for all electrophysiological and imaging experiments. Student's *t* tests were performed in the analysis of spine density, coimmunoprecipitation assays, and Rac1/RhoA activity assays. Sample sizes for all experiments are consistent with those reported in the literature. For all statistical analysis, p values of <0.05 (indicated by *) were considered significant and data are presented as mean ± SEM throughout the study.

Results

The ASD/ID-related mutation Trio N1080I disrupts Trio protein function and blocks synaptogenesis mediated by the ASD/ID-related mutation Trio D1368V

We recently discovered a large cluster of disruptive ASD/ID-related *de novo* mutations in Trio's Rac1-activating domain, GEF1 (Fig. 1*A*) (Sadybekov et al., 2017). Outside of increased Rac1 activation, the molecular mechanism supporting the synaptogenic properties of the hyperfunctional mutation Trio D1368V remains unknown. This is because of our very limited current understanding of the glutamatergic synapse regulatory pathways that involve Trio. Interestingly, ASD/ID-related *de novo* mutations also reside outside of Trio's GEF domains (Fig. 1*A*). Such mutations likely impact protein–protein interactions that govern Trio's influence on glutamatergic synapses. One ASD/ID-related *de novo* missense mutation, Trio N1080I, resides within Trio's eighth spectrin repeat (Fig. 1*A*) and was identified in an individual with severe phenotypes, including no verbal communication, hand stereotypies, and aggressive episodes (Pengelly et al., 2016). We were therefore interested in studying Trio N1080I in an effort to better understand the importance of this spectrin repeat in synaptic function and to uncover the molecular mechanism(s) that are disrupted by this ASD/ID-related mutation. We first generated the N1080I mutation in Trio-9, the most abundant Trio isoform in the brain (McPherson et al., 2005; Portales-Casamar et al., 2006). In order to determine the impact of Trio-9 N1080I on synaptic function, we expressed Trio-9 N1080I in CA1 pyramidal neurons of organotypic rat hippocampal slice cultures using biolistic transfection. Six days after transfection, we recorded evoked AMPAR and NMDAR excitatory postsynaptic currents (AMPAR- and NMDAR-eEPSCs) from Trio-9 N1080I transfected neurons and neighboring untransfected (WT) neurons simultaneously during stimulation of Schaffer collaterals (Fig. 1*B*). This approach permits a pairwise, internally controlled comparison of the consequences of the genetic manipulation (Herring and Nicoll, 2016; Paskus et al., 2019; Rao et al., 2019). We have shown previously that overexpression of Trio-9 produces a twofold increase in AMPAR-eEPSC amplitude (Fig. 1*C*) (Sadybekov et al., 2017). In contrast, expression of Trio-9 N1080I failed to increase the amplitude of AMPAR-eEPSCs (Fig. 1*C*,*D*). NMDAR-eEPSC amplitude was not affected by expression of either Trio-9 or Trio-9 N1080I (Fig. 1*C*,*D*). These data demonstrate that, in neurons, Trio N1080I inhibits Trio's influence on glutamatergic synapse function.

We have previously shown that, in contrast to WT Trio-9, expression of the hyperfunctional ASD/ID-related Trio mutant, Trio-9 D1368V, in CA1 pyramidal neurons markedly increases dendritic spine density as well as both AMPAR- and NMDAR-eEPSC amplitude (Sadybekov et al., 2017). One possibility is that the increased Rac1 activation caused by the D1368V mutation amplifies a synaptogenic regulatory pathway involving Trio. It stands to reason that Trio's involvement in such a synaptogenic regulatory pathway may be mediated by Trio's association with upstream synaptogenic proteins through its spectrin repeat region. Given the importance of Trio's eighth spectrin repeat in Trio function, its implication in ASD/ID, and potential to support protein–protein interactions, we were interested in whether disruption of this domain by Trio N1080I might prevent Trio's interaction with an upstream synaptogenic protein and prevent Trio D1368V's ability to form new glutamatergic synapses. As shown previously, we find here that expression of Trio-9 D1368V in CA1 pyramidal neurons for 6 d leads to a nearly fivefold increase in AMPAR-eEPSC amplitude (Fig. 1*C*, *D*), an ~3.5-fold increase in NMDAR-eEPSC amplitude (Fig. 1*C*,*D*), and a significant increase in dendritic spine density (Fig. 1*E*). We then introduced the N1080I mutation into Trio-9 D1368V generating a mutant form of Trio-9 harboring both the D1368V mutation and the N1080I mutation. Remarkably, we found that adding the N1080I mutation to Trio-9 D1368V completely blocked Trio-9 D1368V's ability to increase both AMPAR- and NMDAR-eEPSC amplitude (Fig. 1*C*,*D*) and its ability to increase dendritic spine density (Fig. 1*E*). We find that the Trio-9 N1080I mutation does not affect the ability of Trio-9's GEF1 domain to activate Rac1 (Fig. 1*F*). The Trio-9 N1080I mutation also did not alter the limited RhoA activation produced by Trio-9's autoinhibited DH2 domain (Fig. 1*F*) (Lutz et al., 2007). Together, such data suggest that Trio N1080I prevents a protein–protein interaction that is required for Trio D1368V-mediated synaptogenesis.

Trio N1080I inhibits Trio's interaction with NLGN1 and blocks NLGN1-mediated synaptogenesis

We recently found that Trio and its paralog Kalirin bind to NLGN1, a prominent driver of glutamatergic synapse formation (Chubykin et al., 2007; Shipman et al., 2011; Bemben et al., 2014; Paskus et al., 2019). To confirm Trio's interaction with NLGN1 in the brain, we performed an immunoprecipitation assay of endogenous Trio from the P2 fraction of whole rat brain homogenates. Indeed, our coimmunoprecipitation assay revealed that Trio interacts with NLGN1 at synapses *in vivo* (Fig. 2*A*). The absence of Trio binding to another synaptic protein, synaptophysin, in this assay revealed that Trio's interaction with NLGN1 was specific (Fig. 2*A*). Immunoprecipitation of Trio-9 with NLGN1 in HEK293 cells strongly suggests that a direct interaction exists between these two proteins (Fig. 2*B*). We then reasoned that Trio-9 N1080I's ability to prevent Trio-9 D1368V-mediated glutamatergic synaptogenesis may stem from Trio N1080I inhibiting an interaction between Trio and NLGN1. To test this hypothesis, we coexpressed Trio-9 N1080I and NLGN1 in HEK293 cells. Remarkably, we found that NLGN1's ability to

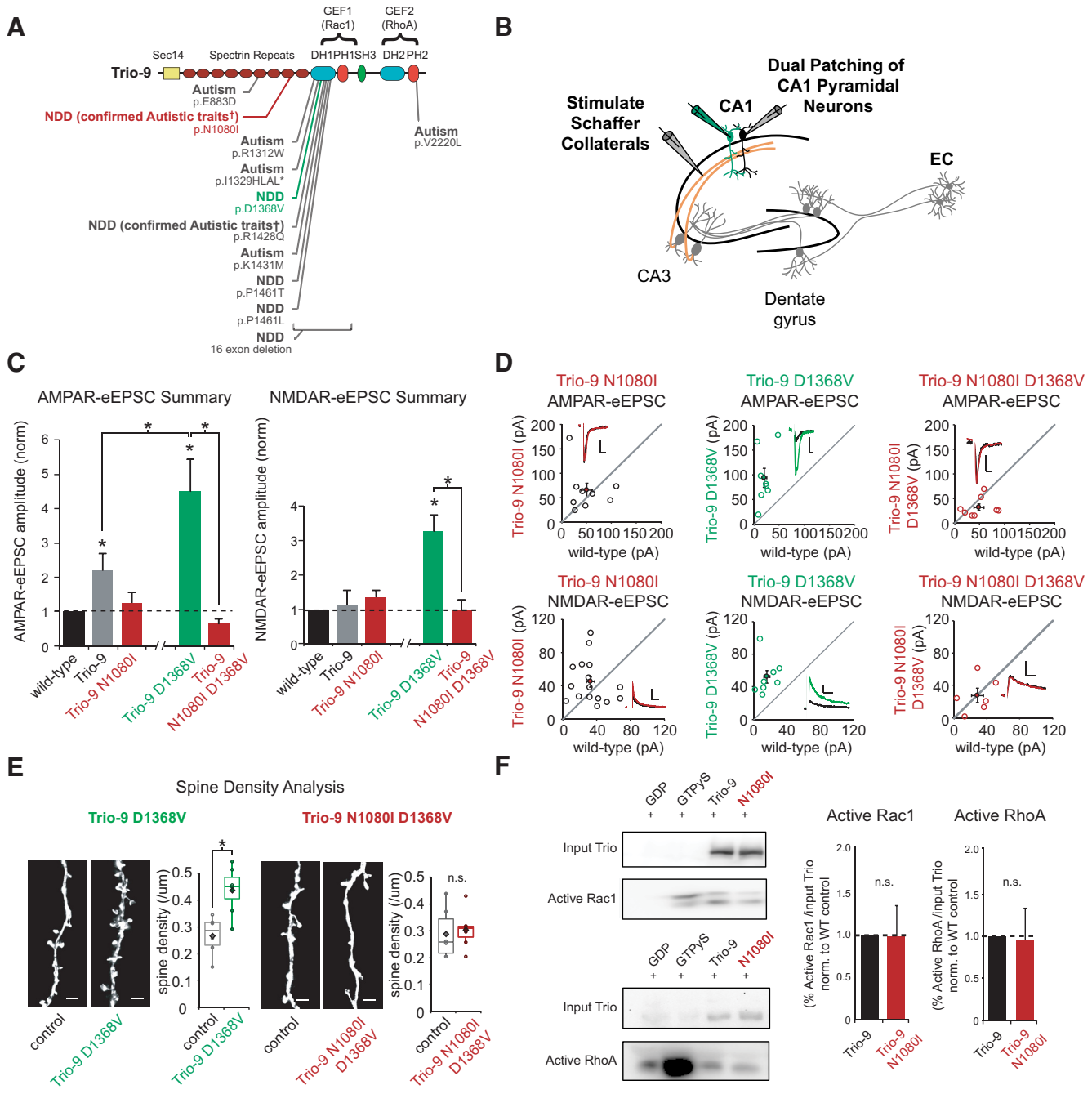

Figure 1. The ASD/ID-related mutation Trio-9 N1080I disrupts Trio protein function and blocks synaptogenesis mediated by the ASD/ID-related mutation Trio-9 D1368V. ***A***, ASD/ID-related *de novo* mutations in Trio. NDD, Neurodevelopmental disorder. †https://decipher.sanger.ac.uk. ***B***, Electrophysiology recording setup. ***C***, Summary of AMPAR- and NMDAR-eEPSC amplitudes (mean ± SEM) for each condition tested normalized to their respective neighboring untransfected paired control neurons (black bar). Significance was determined by Wilcoxon Signed Rank Test in each condition. Gray bars showing the effects of WT Trio-9 overexpression on AMPAR- and NMDAR-eEPSC amplitude represent previously published data (Herring and Nicoll, 2016) and are repeated here for clarity. Trio-9 N1080I expression failed to increase AMPAR-eEPSC amplitude ($n = 9$, $p = 0.8203$). Expression of WT Trio-9 (previously published) or Trio-9 N1080I ($n = 16$, $p = 0.2114$) does not affect NMDAR-eEPSC amplitude. The ASD/ID-related mutant Trio D1368V significantly increased both AMPAR- ($n = 8$, $^*p = 0.0078$) and NMDAR-eEPSC amplitude ($n = 8$, $^*p = 0.0078$). A mutant form of Trio-9 harboring both N1080I and D1368V failed to increase either AMPAR- ($n = 8$, $p = 0.25$) or NMDAR-eEPSC amplitudes ($n = 6$, $p = 1$). Wilcoxon Rank Sum Tests were used to compare across independent conditions (i.e., AMPAR-eEPSCs: WT Trio-9 vs Trio-9 D1368V, $^*p = 0.0093$; Trio-9 N1080I D1368V vs Trio-9 D1368V, $^*p = 0.0003$; NMDAR-eEPSCs: Trio-9 N1080I D1368V vs Trio-9 D1368V, $^*p = 0.0426$). ***D***, Scatterplots showing the data for the individual conditions summarized in ***C***. Open circles represent individual paired recordings. Filled circles represent mean ± SEM. Traces show representative currents for each condition, with the transfected cell in color and the control cell in black (vertical scale bars, 20 pA; horizontal scale bars, 20 ms for AMPA, 50 ms for NMDA). ***E***, Representative dendritic spine images from neurons transfected with Trio-9 D1368V and double mutant Trio-9 N1080I D1368V are shown with their corresponding GFP transfected control dendrites. Scale bars, 2 μm. Boxplots represent the 25th, 50th, and 75th percentiles of each condition with the means (represented by diamonds). Trio-9 D1368V expression resulted in an increase in spine density (Control, $n = 6$; D1368V, $n = 7$; $^*p = 0.0029$, Student's t test). Trio-9 N1080I D1368V expression failed to produce an increase in spine density (Control, $n = 6$; Trio N1080I D1368V, $n = 7$; $p = 0.7452$, Student's t test). ***F***, Trio N1080I has no effect on Trio-9's ability to activate Rac1 ($n = 3$, $p = 0.727$ Student's t test) or RhoA ($n = 3$, $p = 0.842$, Student's t test).

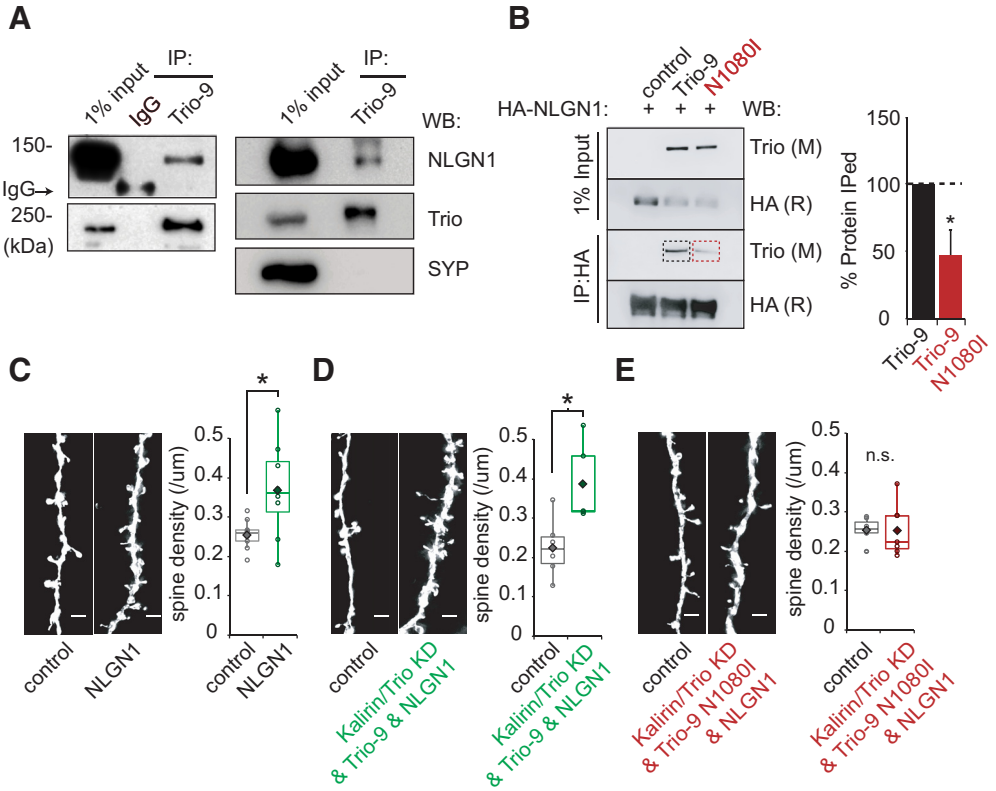

Figure 2. Trio-9 N1080I inhibits Trio's interaction with NLGN1 and blocks NLGN1-mediated synaptogenesis. ***A***, Immunoblots showing coimmunoprecipitation of NLGN1 but not synaptophysin (SYP) with Trio in adult rat P2 brain fractions. ***B***, Left, Immunoblot analysis showing coimmunoprecipitation of HA-NLGN1 with Trio-9 or Trio-9 N1080I in HEK293T cells. Right, Total Trio-9 and Trio-9 N1080I lysate levels (mean ± SEM) normalized to control. Compared with WT Trio, Trio-9 N1080I has significantly less interaction with NLGN1. $*p = 0.02$ (Student's *t* test). ***C–E***, Representative dendritic spine images from transfected neurons of each condition are shown with their corresponding control image. Scale bars, 2 μm. Boxplots represent the 25th, 50th, and 75th percentiles of each condition with the means indicated by diamonds. ***C***, Expression of NLGN1 resulted in an increase in dendritic spine density (control, $n = 9$; NLGN1, $n = 8$). $*p = 0.0192$ (Student's *t* test). ***D***, Replacing endogenous Kalirin and Trio with WT Trio-9 supports a NLGN1-mediated increase in dendritic spine density (control, $n = 6$; Kalirin/Trio KD & Trio-9 & NLGN1, $n = 5$). $*p = 0.0141$ (Student's *t* test). ***E***, Replacing endogenous Kalirin and Trio with Trio-9 N1080I prevented NLGN1 from increasing dendritic spine density (control, $n = 7$; Kalirin/Trio KD & Trio-9 N1080I & NLGN1, $n = 7$). $p = 0.9691$ (Student's *t* test). KD, Knockdown.

coimmunoprecipitate Trio-9 N1080I was significantly reduced by ~50% compared with WT Trio-9 (Fig. 2*B*). Thus, Trio N1080I inhibits Trio's ability to associate with NLGN1.

We next examined whether NLGN1-mediated synaptogenesis is affected by Trio N1080I. NLGN1 is essential in the formation of glutamatergic synapses and expression of NLGN1 in neurons results in a significant increase in dendritic spine density (Chih et al., 2005). We expressed NLGN1 for 6 d in CA1 pyramidal neurons of the hippocampus and found that this resulted in a ~40% increase in spine density compared with control neurons transfected with GFP (Fig. 2*C*). In the brain, both Trio and Kalirin associate with NLGN1; thus, both proteins may support NLGN1's effects on glutamatergic synapse formation. However, Trio is generally expressed in greater abundance than Kalirin in neurons early in postnatal development and stands to play a larger role in supporting NLGN1 effects on glutamatergic synapse formation during this time (McPherson et al., 2002; Ma et al., 2005). In order to isolate the role Trio plays in NLGN1-mediated synaptogenesis and determine whether Trio can support NLGN1-mediated synaptogenesis in the absence of Kalirin, we molecularly replaced endogenous Kalirin and Trio with recombinant Trio-9. We transfected CA1 pyramidal neurons with our previously validated RNAi's against Kalirin and Trio (Herring and Nicoll, 2016), a RNAi-resistant Trio-9 and our NLGN1 expression construct. In these neurons, we observed an increase in dendritic spine density that was nearly identical to NLGN1 overexpression alone in WT neurons (Fig. 2*D*). These results were consistent with Trio-9 supporting NLGN1's ability to create new glutamatergic synapses. In marked contrast, we found that replacing endogenous Trio and Kalirin with Trio-9 N1080I completely abolished NLGN1's ability to increase dendritic spine density (Fig. 2*E*). Together, these data suggest that Trio is sufficient to support NLGN1-mediated synaptogenesis and that inhibiting Trio's ability to associate with NLGN1 prevents NLGN1's ability to promote new glutamatergic synapse formation.

Trio N1080I prevents NLGN1 from increasing NMDAR- but not AMPAR-mediated synaptic transmission

Our observation that Trio-9 N1080I expression prevents NLGN1-mediated increases in dendritic spine number prompted us to perform a detailed electrophysiological examination of how Trio N1080I affects NLGN1's influence on glutamatergic synapse function. In addition to increasing dendritic spine number, synaptogenesis produced by NLGN1 expression is manifested as augmentations of synaptic function (Bemben et al., 2014). For example, we as well as others find that expression of NLGN1 in CA1 pyramidal neurons results in a ~2.5-fold increase in AMPAR- and NMDAR-eEPSC amplitude (Fig. 3*A*,*B*) (Bemben et al., 2014; Paskus et al., 2019). First, to test whether Trio and Kalirin are necessary for NLGN1-mediated increases in AMPAR- and NMDAR-

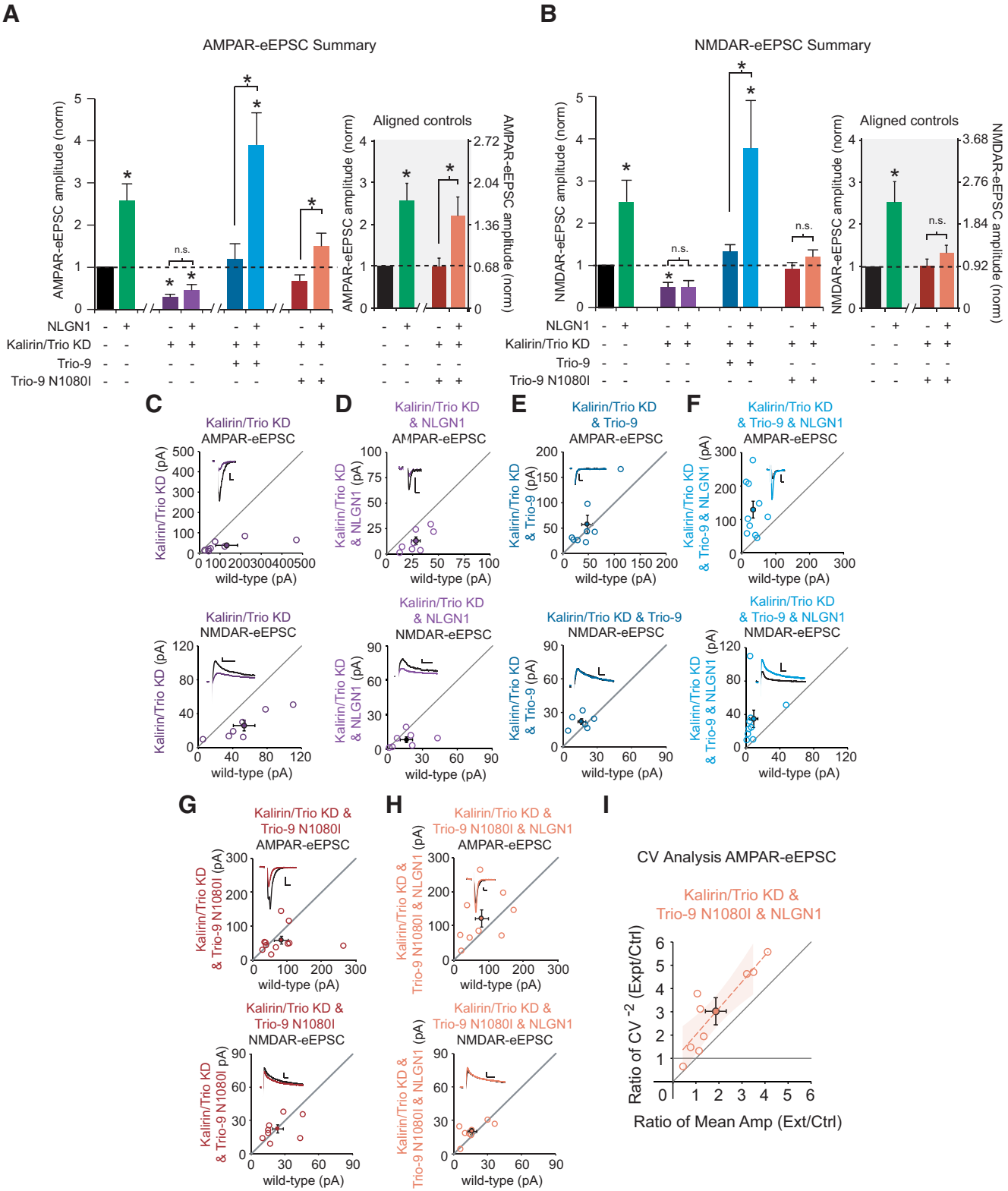

Figure 3. Trio-9 N1080I prevents NLGN1 from increasing NMDAR but not AMPAR-mediated synaptic transmission. Summary of AMPAR- (***A***) and NMDAR-eEPSC (***B***) amplitudes (mean ± SEM) for each condition tested normalized to their neighboring untransfected paired control neurons (black bar). Bar showing the NLGN1 expression phenotype (Paskus et al., 2019) was previously published and is repeated here for clarity. Significance was determined by Wilcoxon Signed Rank Test in each condition. Aligned control graphs represent fold eEPSC amplitude change of NLGN1 expression on the WT background versus the Trio-9 N1080I replacement background. ***C-H***, Scatterplots showing the individual conditions summarized in ***A*** and ***B***. Open circles represent individual paired recordings. Filled circles represent mean ± SEM. Traces show representative currents for each condition, with the transfected cell in color and the control cell in black (vertical scale bars, 20 pA; horizontal scale bars, 20 ms for AMPA, 50 ms for NMDA). ***C***, Knocking down Kalirin and Trio significantly reduced AMPAR- and NMDAR-eEPSC amplitudes (AMPAR-eEPSC, $n = 8$, $^*p = 0.0078$; NMDAR-eEPSC, $n = 7$, $^*p = 0.0312$). ***D***, NLGN1 expression on the Kalirin and Trio double knockdown did not increase either AMPAR-eEPSC or NMDAR-eEPSC amplitude compared with Kalirin and Trio double knockdown (Kalirin/Trio KD & NLGN1: AMPAR-eEPSC, $n = 8$, $^*p = 0.0078$; NMDAR-eEPSC, $n = 7$, $p = 0.2188$; Kalirin/Trio KD vs Kalirin/Trio KD & NLGN1, Wilcoxon Rank Sum Tests: AMPA-eEPSC, $p = 1$, NMDAR-eEPSC, $p = 0.9015$). ***E***, Replacing Kalirin and Trio with WT Trio-9 produced AMPAR- and NMDAR-eEPSC amplitudes that were similar to

eEPSC amplitude, we knocked down both Kalirin and Trio in CA1 pyramidal neurons. As previously published (Herring and Nicoll, 2016), we found here that simultaneous knockdown of Kalirin and Trio results in substantial reductions in AMPAR- and NMDAR-eEPSC amplitude (Fig. 3*A–C*). We then tested the effect of NLGN1 expression on this Kalirin/Trio double knockdown background. We found that simultaneous knockdown of Kalirin and Trio prevented NLGN1-mediated increases in AMPAR- and NMDAR-eEPSC amplitude (Fig. 3*A*,*B*,*D*). These data demonstrate that Kalirin and Trio are required for NLGN1-mediated augmentation of AMPAR- and NMDAR-mediated synaptic transmission.

Given that Kalirin and Trio are paralogous proteins that both interact with NLGN1, we reasoned that Kalirin and Trio should be capable of supporting NLGN1-mediated synaptogenesis independently. We have shown previously that Kalirin alone can support NLGN1-mediated increases in AMPAR- and NMDAR-eEPSC amplitude in the absence of Trio (Paskus et al., 2019). Here, we were interested in whether Trio is able to support NLGN1-mediated increases in AMPAR- and NMDAR-eEPSC amplitude in the absence of Kalirin. To answer this question, we first expressed recombinant Trio-9 on a Trio and Kalirin double knockdown background and found that molecular replacement of Kalirin and Trio with recombinant Trio-9 restored normal glutamatergic transmission (Fig. 3*A*, *B*,*E*). This result is consistent with our previously published results (Herring and Nicoll, 2016) and illustrates that Trio-9 is able to substitute for Kalirin in supporting basal synaptic transmission. We then examined the effect of NLGN1 expression on this Trio-9 replacement background to determine whether NLGN1 can augment glutamatergic synapse function through Trio in the absence of Kalirin. We found that NLGN1 expression on this Trio-9 replacement background produced robust increases in both AMPAR- and NMDAR-eEPSC amplitude compared with both paired untransfected WT neurons and neurons where Kalirin and Trio were molecularly replaced with Trio-9 (Fig. 3*A*,*B*,*F*). These results were consistent with the effects we observed with this genetic manipulation on dendritic spine density (Fig. 2*D*) and demonstrate that Trio is able to support NLGN1-mediated synaptogenesis in the absence of Kalirin.

We were then interested in whether Trio N1080I affects NLGN1's ability to augment glutamatergic neurotransmission. To answer this question, we first cotransfected CA1 pyramidal neurons with our Kalirin and Trio RNAi and our Trio-9 N1080I expression construct. We found that molecularly replacing Kalirin and Trio with Trio-9 N1080I resulted in AMPAR- and NMDAR-eEPSCs that were similar to untransfected neurons (Fig. 3*A*,*B*,*G*). In contrast to molecular replacement with WT Trio, we found that molecular replacement with Trio-9 N1080I completely blocked NLGN1's ability to increase NMDAR-eEPSC amplitude (Fig. 3*B*,*H*). This result was also consistent with the effects we observed with this genetic manipulation on dendritic spine density (Fig. 2*E*), given that NMDAR-eEPSC amplitude phenotypes are often coupled with changes in spine density (Woolley et al., 1997; Herring and Nicoll, 2016; Sadybekov et al., 2017; Tian et al., 2018). However, molecular replacement with Trio-9 N1080I failed to prevent NLGN1's ability to increase AMPAR-eEPSC amplitude. NLGN1 expression on the Trio-9 N1080I replacement background led to a greater than twofold increase in AMPAR-eEPSC amplitude compared with AMPAR-eEPSCs of Trio-9 N1080I replacement neurons that were not transfected with NLGN1 (Fig. 3*A*,*H*). The magnitude of this increase in AMPAR-eEPSC amplitude was nearly identical to that observed when NLGN1 is expressed on a WT background (Fig. 3*A*). Given that this increase in AMPAR-eEPSC amplitude occurred in the absence of increased spine number and NMDAR-eEPSC amplitude, we conclude that AMPAR function is augmented at existing synapses. This increase in AMPAR-eEPSC amplitudes could be because of a reduction in the number of AMPAR-lacking ("silent") glutamatergic synapses, or alternatively because of a uniform modification in AMPAR-mediated synapse transmission across all functional synapses. To determine the source of the increase in AMPAR-eEPSC amplitude when expressing NLGN1 on Trio N1080I replacement background, we performed coefficient of variation (CV) analysis on the AMPAR-eEPSC amplitudes of this condition. CV analysis can be used to determine the quantal parameters of glutamatergic transmission in control and transfected neurons. By comparing the normalized variance in AMPAR-eEPSC amplitudes from two neurons receiving the same stimulus, it is possible to estimate relative quantal size and quantal content (Del Castillo and Katz, 1954; Bekkers and Stevens, 1990; Malinow and Tsien, 1990). Changes in quantal size precisely change both the mean eEPSC and the variance such that the normalized ratio of mean^2/variance, also known as CV (or CV^{-2}), remains constant. Changes in quantal size cause the marker of the mean to fall on the horizontal line seen in Figure 3*I* and, in the context of this preparation, indicate a change in the number of glutamate receptors at all synapses. In contrast, changes in quantal content will produce proportional changes of equal magnitude in CV^{-2} and mean eEPSC amplitudes that cause the marker of the mean to fall close to the diagonal line. Here, changes in quantal content indicate a change in the number of synapses expressing glutamatergic receptors. We observed proportional increases in CV^{-2} and mean AMPAR-eEPSC amplitude following NLGN1 expression on the Trio N1080I molecular replacement background (Fig. 3*I*). This result identified a clear increase in quantal content rather than quantal size as responsible for the increase in AMPAR-eEPSC amplitude we observe. Therefore, we conclude that NLGN1 expression on the Trio N1080I replacement background results in an increase in the number of synapses that contain AMPARs. Together, our results show that the ASD/ID-related mutation Trio N1080I leads to a selective inhibition of

←

paired controls (AMPAR-eEPSCs, $n = 8$, $p = 0.6406$; NMDAR-eEPSCs, $n = 6$, $p = 0.2807$). ***F***, When Kalirin and Trio were replaced by WT Trio-9, expression of NLGN1 increased AMPAR- and NMDAR-eEPSC amplitudes compared with WT controls (AMPAR-eEPSCs, $n = 8$, $^*p = 0.0019$; NMDAR-eEPSCs, $n = 7$, $^*p = 0.0039$) and neurons where Kalirin and Trio were replaced with Trio-9 (AMPAR-eEPSCs, $^*p = 0.0062$; NMDAR-eEPSCs, $^*p = 0.0119$, Wilcoxon Rank Sum Tests). ***G***, Replacing Kalirin and Trio with Trio-9 N1080I produced AMPAR- and NMDAR-eEPSC amplitudes that were similar to paired controls (AMPAR-eEPSCs, $n = 11$, $p = 0.5195$; NMDAR-eEPSCs, $n = 8$, $p = 0.9453$). ***H***, NLGN1 expression on the Trio-9 N1080I replacement background did not increase AMPAR-eEPSC amplitude compared with paired control neurons ($n = 9$, $p = 0.2031$, Wilcoxon Rank Sum Tests) but produced a significant increase relative to replacing Kalirin and Trio with Trio-9 N1080I ($^*p = 0.0465$, Wilcoxon Rank Sum Tests, ***A***). NLGN1 expression on the Trio-9 N1080I replacement background did not affect NMDAR-eEPSC amplitude compared with paired control neurons ($n = 8$, $p = 0.3125$, Wilcoxon Rank Sum Tests) or relative to replacing Kalirin and Trio with Trio-9 N1080I ($p = 0.8785$, Wilcoxon Rank Sum Tests, ***B***). ***I***, CV analysis of AMPAR-eEPSCs from pairs of control neurons and neurons where NLGN1 was expressed on the Trio-9 N1080I molecular replacement background. CV^{-2} ratios are graphed against the mean amplitude ratio for each pair. Filled circles represent mean ± SEM. Dashed lines indicate linear regression. Highlighted region represents 95% CI (Kalirin/Trio KD & Trio N1080I & NLGN1, $n = 9$ pairs, $R^2 = 0.787$, $^*p = 0.0014$, Simple Linear Regression). KD, Knockdown.

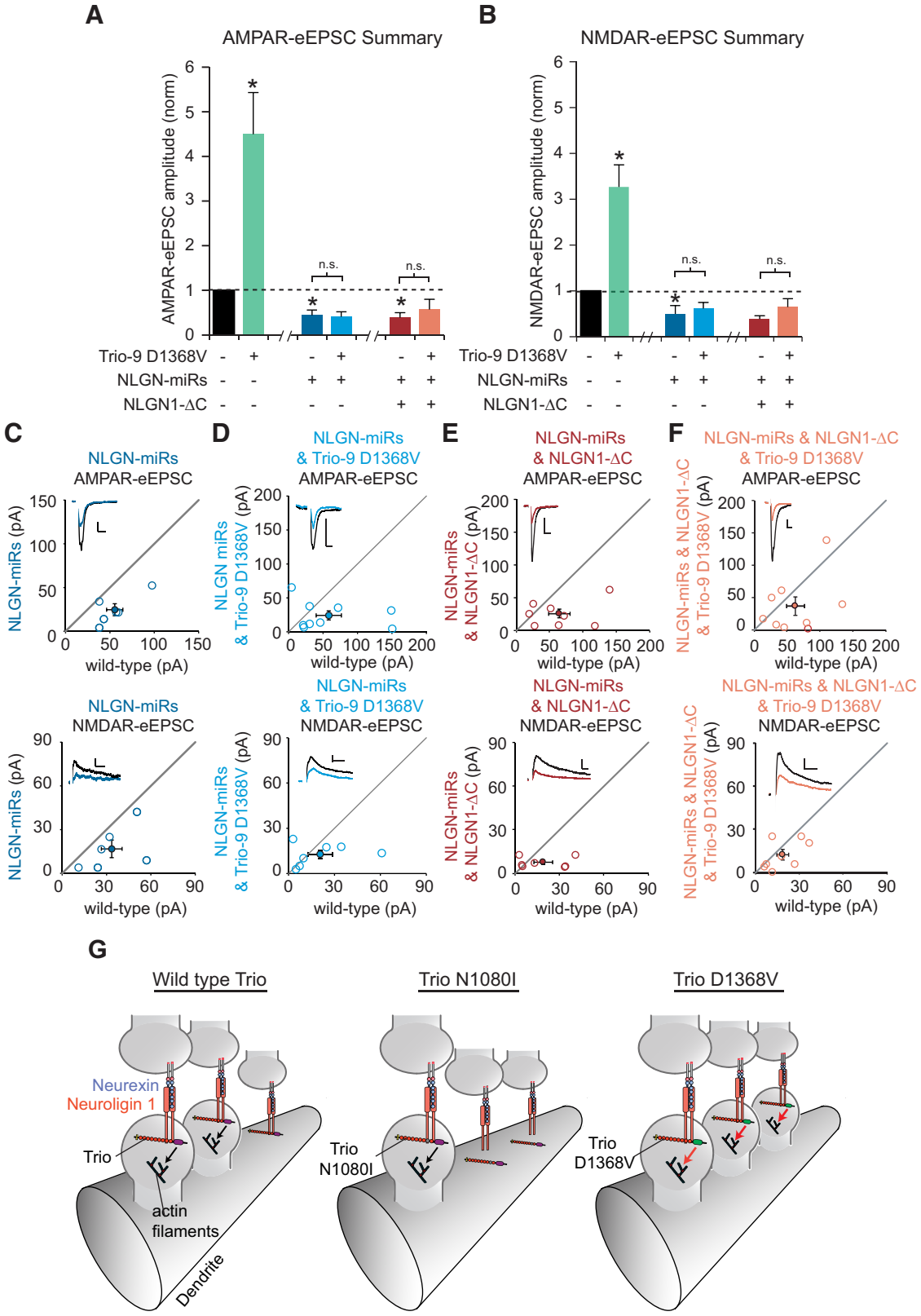

Figure 4. NLGN signaling is required for Trio-9 D1368V-mediated synaptogenesis. Summary of AMPAR (***A***) and NMDAR-eEPSC (***B***) amplitudes (mean ± SEM) for each condition tested normalized to their neighboring untransfected paired control neurons (black bar). Bars for the Trio-9 D1368V expression phenotype are shown in Figure 1 and are repeated here for clarity. Significance was determined by Wilcoxon Signed Rank Test in each condition (AMPAR-eEPSCs: NLGN-miRs, $n = 6$, $^*p = 0.0313$; NLGN-miRs & Trio-9 D1368V, $n = 9$, $p = 0.0977$; NLGN miRs & NLGN1-ΔC, $n = 7$, $^*p = 0.0390$; NLGN-miRs & NLGN1-ΔC & Trio-9 D1368V, $n = 9$, $p = 0.2031$; NMDAR-eEPSCs: NLGN-miRs, $n = 6$, $^*p = 0.0355$; NLGN-miRs & Trio-9 D1368V, $n = 7$, $p = 0.2969$; NLGN-miRs & NLGN1-ΔC, $n = 6$, $p = 0.2188$; NLGN-miRs & NLGN1-ΔC & Trio-9 D1368V, $n = 8$, $p = 0.1094$). Expression of Trio-9 D1368V did not increase AMPAR- or NMDAR-eEPSC amplitude on the NLGN-miRs background (AMPAR-eEPSC, $p = 1$; NMDAR-eEPSC, $p = 0.366$, Wilcoxon Rank Sum Tests) or on the NLGN1-ΔC replacement background (AMPAR-eEPSC, $p = 0.9626$; NMDAR-eEPSC, $p = 0.9551$, Wilcoxon Rank Sum Tests). ***C–F***, Scatterplots showing the individual conditions summarized in ***A*** and ***B***. Open circles represent individual paired recordings. Filled circles represent mean ± SEM. Traces show representative currents for each condition, with the transfected cell in color and the control cell in black (vertical scale bars, 20 pA;

NLGN1's ability to create new synapses while preserving the ability of NLGN1 to convert AMPAR lacking silent synapses into AMPAR-containing functional synapses.

NLGN signaling is required for Trio D1368V-mediated synaptogenesis

Above we show that the ASD/ID-related mutation Trio N1080I inhibits NLGN1's association with Trio-9. We also show that the Trio N1080I mutation prevents the synaptogenesis caused by the hyperfunctional ASD/ID-related mutation Trio D1368V. Together, these data are consistent with the idea that Trio D1368V pathologically increases glutamatergic synapse formation by amplifying NLGN1-mediated synaptogenesis. If NLGN1 signaling is indeed required for the pathologic synapse formation produced by Trio D1368V, knocking down NLGN1 should prevent Trio D1368V from enhancing glutamatergic synapse function. Because of overlapping function, the presence of other NLGN isoforms is believed to compensate for the elimination of individual NLGN isoforms at synapses (Shipman et al., 2011; Shipman and Nicoll, 2012). Thus, elimination of the three major Neuroligin proteins (NLGN1-NLGN3) that influence synaptic formation using a chained NLGN1-NLGN3 miRNA construct (NLGN-miRs) has been used to study the role of NLGN signaling in neurons (Shipman et al., 2011; Shipman and Nicoll, 2012; Bemben et al., 2014). It has been shown previously that knockdown of NLGN1-NLGN3 in CA1 pyramidal neurons results in a reduction in glutamatergic neurotransmission (Shipman et al., 2011). Consistent with this study, we find that expressing the chained NLGN-miRs construct in CA1 pyramidal neurons reduced both AMPAR- and NMDAR-eEPSC amplitude (Fig. 4*A–C*). We then expressed Trio-9 D1368V on this NLGN knockdown background and asked whether expression of Trio-9 D1368V enhances glutamatergic synapse transmission in the absence of NLGN protein function. We observed a similar reduction in both AMPAR- and NMDAR-eEPSC amplitude compared with NLGN1-NLGN3 knockdown (Fig. 4*A*,*B*,*D*). These data demonstrate that NLGN signaling is required for Trio-9 D1368V to induce the generation of new synapses.

As cell adhesion molecules, NLGN proteins are composed of an extracellular domain, a transmembrane domain, and intracellular cytoplasmic terminal (C-tail) domain, with the extracellular domain being critical for NLGN protein interactions with presynaptic Neurexin proteins. In order to investigate whether NLGN1 intracellular signaling is specifically required for the synapse formation produced by Trio-9 D1368V, we expressed a form of NLGN1 lacking its intracellular C-tail domain (NLGN1-ΔC) together with the NLGN-miRs. This molecular replacement of endogenous NLGN1-NLGN3 proteins with NLGN C-tail mutations was shown previously to be necessary for isolating and studying the effects of NLGN C-tail truncation mutations on synaptic function (Shipman et al., 2011). We find that NLGN1-ΔC molecular replacement resulted in reduced glutamatergic synaptic transmission that was similar to the NLGN miRs alone (Fig. 4*A*,*B*,*E*), demonstrating an elimination of NLGN1 signaling in these neurons. We then expressed Trio-9 D1368V on this NLGN1-ΔC molecular replacement background and asked whether expression of Trio-9 D1368V could still enhance AMPAR- and NMDAR-eEPSC amplitude. Similar to expression of D1368V on NLGN knockdown background, we observed no significant difference between NLGN1-ΔC molecular replacement and expression of Trio-9 D1368V on the NLGN1-ΔC molecular replacement background (Fig. 4*A*,*B*,*F*). Together, our results demonstrate that NLGN intracellular signaling is required for Trio D1368V-mediated synaptogenesis.

Discussion

Disruption of glutamatergic neurotransmission is widely believed to underlie the development of ASD/ID-related disorders (Rojas, 2014; Bourgeron, 2015; Volk et al., 2015). Trio resides within dendritic spines where it promotes actin polymerization through its ability to activate Rac1 (Herring and Nicoll, 2016; Sadybekov et al., 2017; Paskus et al., 2019). This function is critical for the formation and maintenance of glutamatergic synapses in the brain. The majority of ASD/ID-related mutations identified in Trio are clustered in Trio's GEF1 domain and alter Trio's ability to activate Trio's downstream effector molecule Rac1. The ASD/ID-related mutation Trio D1368V increases Trio's ability to activate Rac1 and produces a potentially pathologic increase in glutamatergic synapse formation. These data suggest that Trio is coupled to molecular mechanisms that govern glutamatergic synapse formation. However, before this study, the molecular mechanisms responsible for Trio D1368V-mediated synaptogenesis have not been explored. The spectrin repeat region of Trio likely supports protein–protein interactions that govern Trio's involvement in specific neuronal regulatory processes. We reasoned that this region may support an interaction between Trio and proteins that promote glutamatergic synapse formation. Another ASD/ID-related Trio mutation, Trio N1080I, is located in Trio's eighth spectrin repeat and inhibits Trio function without affecting Trio's ability to activate small GTPases. Remarkably, we found that a mutant form of Trio harboring both the N1080I and D1368V mutations does not increase glutamatergic synapse formation. These data are consistent with the N1080I mutation preventing Trio's association with proteins involved in glutamatergic synaptogenesis, and thus precluding Trio D1368V-mediated elevations in Rac1 signaling from making more synapses.

Trio and its paralog Kalirin interact with NLGN1, a postsynaptic protein that promotes glutamatergic synaptogenesis through its interaction with presynaptic neurexin proteins. NLGN1 overexpression in neurons increases dendritic spine number and produces large increases in AMPAR- and NMDAR-mediated synaptic currents. We have shown previously that Kalirin can support NLGN1 function in the absence of Trio (Paskus et al., 2019). Here, we now show that Trio can support NLGN1 function in the absence of Kalirin (Fig. 4*G*). These data provide additional evidence that Trio and Kalirin play overlapping roles in the regulation of postsynaptic function. However, Trio is generally expressed at higher levels than Kalirin early in postnatal development with Kalirin expression peaking later in development (McPherson et al., 2002; Ma et al., 2003, 2005). Thus, the influence Trio and Kalirin have on synaptic regulation may vary as the brain develops. It is currently unknown why the brain utilizes Trio over Kalirin at early developmental time

←

horizontal scale bars, 20 ms for AMPA, 50 ms for NMDA). ***G***, Model illustrations: NLGN1 promotes synaptogenesis through its interaction with Trio; Trio N1080I inhibits Trio's interaction with NLGN1 and prevents NLGN1-mediated synaptogenesis; Trio D1368V augments NLGN1-mediated synaptogenesis through increased Rac1-mediated actin polymerization. KD, Knockdown.

points. Going forward, it will be important to identify the specialized roles these proteins play in synaptic regulation.

In the present study, we find that the Trio N1080I inhibits Trio's ability to interact with NLGN1. In contrast to WT Trio, we find that molecular replacement of Kalirin and Trio with Trio-9 N1080I prevented NLGN1 expression from increasing dendritic spine number and synaptic NMDAR-mediated current amplitude. Thus, Trio-9 N1080I prevents NLGN1 from creating new synapses. Surprisingly, Trio N1080I molecular replacement did not prevent NLGN1's ability to increase synaptic AMPAR-mediated current amplitude. Such data suggest that Trio N1080I may contribute to the development of ASD/ID by uncoupling NLGN1's effects on glutamatergic synapses, with this mutation selectively preventing NLGN1-mediated synaptogenesis but leaving NLGN1's ability to increase synaptic AMPAR function at existing synapses intact (Fig. 4*G*). Given that Trio N1080I does not completely prevent Trio's ability to interact with NLGN1, we believe that NLGN1's ability to increase synaptic AMPAR function is supported by Trio N1080I. Stronger interactions between Trio and NLGN1 may be required for NLGN1-mediated synaptogenesis given the larger cytoplasmic volume of the dendrites relative to existing synapses. The smaller cytoplasmic volume of existing synapses may result in higher Trio N1080I concentrations relative to dendrites and allow functional NLGN1-Trio N1080I interactions to occur within these structures. However, it is alternatively possible that NLGN1 increases synaptic AMPAR function at existing synapses via a Trio-independent mechanism. We believe this explanation is less likely given that eliminating Kalirin and Trio expression prevents NLGN1-mediated increases in both AMPAR and NMDAR function.

The ASD/ID-related mutation Trio-9 D1368V increases the ability of Trio-9 to activate Rac1 and results in aberrant synaptogenic qualities not observed with WT Trio-9. In the present study, we show that Trio-9 D1368V-mediated synaptogenesis is blocked by inhibiting Trio's interaction with NLGN1 via N1080I. We also show that Trio-9 D1368V-mediated synaptogenesis is blocked by eliminating intracellular NLGN signaling in neurons. Therefore, we conclude that the synaptogenesis produced by Trio-9 D1368V is mediated through a pathologic increase in NLGN1-mediated glutamatergic synapse formation (Fig. 4*G*). While Trio D1368V-mediated synaptogenesis relies on NLGN signaling, it is interesting that molecular replacement of Kalirin and Trio with Trio-9 N1080I largely restores baseline glutamatergic neurotransmission. This finding is consistent with our previous study in which a form of Kalirin that is unable to bind to NLGN1 is able to support largely normal baseline synaptic transmission (Paskus et al., 2019). Such data may be explained by Kalirin and Trio interacting with other NLGN isoforms or other postsynaptic trans-synaptic adhesion complex proteins which compensate for reduced Kalirin and Trio binding to NLGN1. Given that deficits in glutamatergic neurotransmission are only observed when NLGN1 expression is reduced during late embryonic development (Shipman and Nicoll, 2012), it is possible that deficits in baseline synaptic transmission resulting from the Trio N1080I mutation only arise transiently during periods of robust NLGN1-specific synaptogenesis during the earliest phases of synaptic development. Going forward, it will be important to test this hypothesis in animal models harboring the Trio N1080I mutation.

This work now provides examples of ASD/ID-related mutations in Trio that are able to augment as well as inhibit NLGN-mediated signaling in neurons. Thus, either strengthening or weakening this newly identified synaptic regulatory pathway stands to produce alterations in glutamate-mediated synaptic communication between neurons that contribute to the development of ASD/ID-related disorders. As a result, the development of therapeutics targeting NLGN1/Trio-mediated glutamatergic synapse regulation may be a useful strategy in treating ASD/ID. In addition to NLGN1, our proteomic work has revealed interactions between Trio and other ASD-related genes as well (e.g., CTTNBP2, CRMP1, and DPYSL2) (Paskus et al., 2019). Future investigation of the interactions between Trio and such ASD-linked proteins will be essential to our understanding of how Trio dysfunction contributes to the development ASD/ID-related disorders.

References

Barbosa S, Greville-Heygate S, Bonnet M, Godwin A, Fagotto-Kaufmann C, Kajava AV, Laouteouet D, Mawby R, Wai HA, Dingemans AJM, Hehir-Kwa J, Willems M, Capri Y, Mehta SG, Cox H, Goudie D, Vansenne F, Turnpenny P, Vincent M, Cogne B (2020) Opposite modulation of Rac1 by mutations in TRIO is associated with distinct, domain-specific neurodevelopmental disorders. Am J Hum Genet 106:338–355.

Bekkers JM, Stevens CF (1990) Presynaptic mechanism for long-term potentiation in the hippocampus. Nature 346:724–729.

Bellanger JM, Astier C, Sardet C, Ohta Y, Stossel TP, Debant A (2000) The Rac1- and RhoG-specific GEF domain of Trio targets filamin to remodel cytoskeletal actin. Nat Cell Biol 2:888–892.

Bemben MA, Shipman SL, Hirai T, Herring BE, Li Y, Badger JD 2nd, Nicoll RA, Diamond JS, Roche KW (2014) CaMKII phosphorylation of neuroligin-1 regulates excitatory synapses. Nat Neurosci 17:56–64.

Bemben MA, Shipman SL, Nicoll RA, Roche KW (2015) The cellular and molecular landscape of neuroligins. Trends Neurosci 38:496–505.

Blundell J, Blaiss CA, Etherton MR, Espinosa F, Tabuchi K, Walz C, Bolliger MF, Südhof TC, Powell CM (2010) Neuroligin-1 deletion results in impaired spatial memory and increased repetitive behavior. J Neurosci 30:2115–2129.

Bourgeron T (2015) From the genetic architecture to synaptic plasticity in autism spectrum disorder. Nat Rev Neurosci 16:551–563.

Chih B, Engelman H, Scheiffele P (2005) Control of excitatory and inhibitory synapse formation by neuroligins. Science 307:1324–1328.

Chubykin AA, Atasoy D, Etherton MR, Brose N, Kavalali ET, Gibson JR, Sudhof TC (2007) Activity-dependent validation of excitatory versus inhibitory synapses by neuroligin-1 versus neuroligin-2. Neuron 54:919–931.

Comery TA, Harris JB, Willems PJ, Oostra BA, Irwin SA, Weiler IJ, Greenough WT (1997) Abnormal dendritic spines in fragile X knockout mice: maturation and pruning deficits. Proc Natl Acad Sci USA 94:5401–5404.

De Rubeis S, He X, Goldberg AP, Poultney CS, Samocha K, Ercument Cicek A, Kou Y, Liu L, Fromer M, Walker S, Singh T, Klei L, Kosmicki J, Fu SC, Aleksic B, Biscaldi M, Bolton PF, Brownfeld JM, Cai J, Campbell NG, et al. (2014) Synaptic, transcriptional and chromatin genes disrupted in autism. Nature 515:209–215.

Del Castillo J, Katz B (1954) Quantal components of the end-plate potential. J Physiol 124:560–573.

Djinovic-Carugo K, Gautel M, Ylänne J, Young P (2002) The spectrin repeat: a structural platform for cytoskeletal protein assemblies. FEBS Lett 513:119–123.

Dolan BM, Duron SG, Campbell DA, Vollrath B, Shankaranarayana Rao BS, Ko HY, Lin GG, Govindarajan A, Choi SY, Tonegawa S (2013) Rescue of fragile X syndrome phenotypes in Fmr1 KO mice by the small-molecule PAK inhibitor FRAX486. Proc Natl Acad Sci USA 110:5671–5676.

Duffney LJ, Zhong P, Wei J, Matas E, Cheng J, Qin L, Ma K, Dietz DM, Kajiwara Y, Buxbaum JD, Yan Z (2015) Autism-like deficits in Shank3-deficient mice are rescued by targeting actin regulators. Cell Rep 11:1400–1413.

Forrest MP, Parnell E, Penzes P (2018) Dendritic structural plasticity and neuropsychiatric disease. Nat Rev Neurosci 19:215–234.

Gray JA, Shi Y, Usui H, During MJ, Sakimura K, Nicoll RA (2011) Distinct modes of AMPA receptor suppression at developing synapses by GluN2A and GluN2B: single-cell NMDA receptor subunit deletion in vivo. Neuron 71:1085-1101.

Guo D, Peng Y, Wang L, Sun X, Wang X, Liang C, Yang X, Li S, Xu J, Ye WC, Jiang B, Shi L (2021) Autism-like social deficit generated by Dock4 deficiency is rescued by restoration of Rac1 activity and NMDA receptor function. Mol Psychiatry 26:1505–1519.

Herring BE, Nicoll RA (2016) Kalirin and Trio proteins serve critical roles in excitatory synaptic transmission and LTP. Proc Natl Acad Sci USA 113:2264–2269.

Hutsler JJ, Zhang H (2010) Increased dendritic spine densities on cortical projection neurons in autism spectrum disorders. Brain Res 1309:83–94.

Irwin SA, Patel B, Idupulapati M, Harris JB, Crisostomo RA, Larsen BP, Kooy F, Willems PJ, Cras P, Kozlowski PB, Swain RA, Weiler IJ, Greenough WT (2001) Abnormal dendritic spine characteristics in the temporal and visual cortices of patients with fragile-X syndrome: a quantitative examination. Am J Med Genet 98:161–167.

Joensuu M, Lanoue V, Hotulainen P (2018) Dendritic spine actin cytoskeleton in autism spectrum disorder. Prog Neuropsychopharmacol Biol Psychiatry 84:362–381.

Katrancha SM, Shaw JE, Zhao AY, Myers SA, Cocco AR, Jeng AT, Zhu M, Pittenger C, Greer CA, Carr SA, Xiao X, Koleske AJ (2019) Trio haploinsufficiency causes neurodevelopmental disease-associated deficits. Cell Rep 26:2805–2817.e2809.

Kay Y, Herring BE (2021) An optogenetic method for investigating presynaptic molecular regulation. Sci Rep 11:11329.

Lutz S, Shankaranarayanan A, Coco C, Ridilla M, Nance MR, Vettel C, Baltus D, Evelyn CR, Neubig RR, Wieland T, Tesmer JJ (2007) Structure of Galphaq-p63RhoGEF-RhoA complex reveals a pathway for the activation of RhoA by GPCRs. Science 318:1923–1927.

Ma XM, Huang J, Wang Y, Eipper BA, Mains RE (2003) Kalirin, a multifunctional Rho guanine nucleotide exchange factor, is necessary for maintenance of hippocampal pyramidal neuron dendrites and dendritic spines. J Neurosci 23:10593–10603.

Ma XM, Huang JP, Eipper BA, Mains RE (2005) Expression of Trio, a member of the Dbl family of Rho GEFs in the developing rat brain. J Comp Neurol 482:333–348.

Malinow R, Tsien RW (1990) Presynaptic enhancement shown by whole-cell recordings of long-term potentiation in hippocampal slices. Nature 346:177–180.

Martinez-Cerdeno V (2017) Dendrite and spine modifications in autism and related neurodevelopmental disorders in patients and animal models. Dev Neurobiol 77:393–404.

McPherson CE, Eipper BA, Mains RE (2002) Genomic organization and differential expression of Kalirin isoforms. Gene 284:41–51.

McPherson CE, Eipper BA, Mains RE (2005) Multiple novel isoforms of Trio are expressed in the developing rat brain. Gene 347:125–135.

Nakanishi M, Nomura J, Ji X, Tamada K, Arai T, Takahashi E, Bucan M, Takumi T (2017) Functional significance of rare neuroligin 1 variants found in autism. PLoS Genet 13:e1006940.

Paskus JD, Tian C, Fingleton E, Shen C, Chen X, Li Y, Myers SA, Badger JD, Bemben MA, Herring BE, Roche KW (2019) Synaptic kalirin-7 and trio interactomes reveal a GEF protein-dependent neuroligin-1 mechanism of action. Cell Rep 29:2944–2952.e2945.

Paskus JD, Herring BE, Roche KW (2020) Kalirin and Trio: RhoGEFs in Synaptic Transmission, Plasticity, and Complex Brain Disorders. Trends Neurosci 43:505–518.

Pengelly RJ, Greville-Heygate S, Schmidt S, Seaby EG, Jabalameli MR, Mehta SG, Parker MJ, Goudie D, Fagotto-Kaufmann C, Mercer C, Debant A, Ennis S, Baralle D, DDD Study (2016) Mutations specific to the Rac-GEF domain of TRIO cause intellectual disability and microcephaly. J Med Genet 53:735–742.

Penzes P, Jones KA (2008) Dendritic spine dynamics: a key role for kalirin-7. Trends Neurosci 31:419–427.

Penzes P, Remmers C (2012) Kalirin signaling: implications for synaptic pathology. Mol Neurobiol 45:109–118.

Penzes P, Johnson RC, Sattler R, Zhang X, Huganir RL, Kambampati V, Mains RE, Eipper BA (2001) The neuronal Rho-GEF Kalirin-7 interacts with PDZ domain-containing proteins and regulates dendritic morphogenesis. Neuron 29:229–242.

Portales-Casamar E, Briancon-Marjollet A, Fromont S, Triboulet R, Debant A (2006) Identification of novel neuronal isoforms of the Rho-GEF Trio. Biol Cell 98:183–193.

Rao S, Kay Y, Herring BE (2019) Tiam1 is critical for glutamatergic synapse structure and function in the hippocampus. J Neurosci 39:9306–9315.

Rojas DC (2014) The role of glutamate and its receptors in autism and the use of glutamate receptor antagonists in treatment. J Neural Transm (Vienna) 121:891–905.

Sadybekov A, Tian C, Arnesano C, Katritch V, Herring BE (2017) An autism spectrum disorder-related de novo mutation hotspot discovered in the GEF1 domain of Trio. Nat Commun 8:601.

Schenck A, Bardoni B, Langmann C, Harden N, Mandel JL, Giangrande A (2003) CYFIP/Sra-1 controls neuronal connectivity in *Drosophila* and links the Rac1 GTPase pathway to the Fragile X protein. Neuron 38:887–898.

Schnell E, Sizemore M, Karimzadegan S, Chen L, Bredt DS, Nicoll RA (2002) Direct interactions between PSD-95 and stargazin control synaptic AMPA receptor number. Proc Natl Acad Sci USA 99:13902–13907.

Shipman SL, Nicoll RA (2012) A subtype-specific function for the extracellular domain of neuroligin 1 in hippocampal LTP. Neuron 76:309–316.

Shipman SL, Schnell E, Hirai T, Chen BS, Roche KW, Nicoll RA (2011) Functional dependence of neuroligin on a new non-PDZ intracellular domain. Nat Neurosci 14:718–726.

Stoppini L, Buchs PA, Muller D (1991) A simple method for organotypic cultures of nervous tissue. J Neurosci Methods 37:173–182.

Tang G, Gudsnuk K, Kuo SH, Cotrina ML, Rosoklija G, Sosunov A, Sonders MS, Kanter E, Castagna C, Yamamoto A, Yue Z, Arancio O, Peterson BS, Champagne F, Dwork AJ, Goldman J, Sulzer D (2014) Loss of mTOR-dependent macroautophagy causes autistic-like synaptic pruning deficits. Neuron 83:1131–1143.

Tian C, Kay Y, Sadybekov A, Rao S, Katritch V, Herring BE (2018) An intellectual disability-related missense mutation in Rac1 prevents LTP induction. Front Mol Neurosci 11:223.

Volk L, Chiu SL, Sharma K, Huganir RL (2015) Glutamate synapses in human cognitive disorders. Annu Rev Neurosci 38:127–149.

Woolley CS, Weiland NG, McEwen BS, Schwartzkroin PA (1997) Estradiol increases the sensitivity of hippocampal CA1 pyramidal cells to NMDA receptor-mediated synaptic input: correlation with dendritic spine density. J Neurosci 17:1848–1859.

Xiang Z, Greenwood AC, Kairiss EW, Brown TH (1994) Quantal mechanism of long-term potentiation in hippocampal mossy-fiber synapses. J Neurophysiol 71:2552–2556.

Zeidán-Chuliá F, Rybarczyk-Filho JL, Salmina AB, de Oliveira BH, Noda M, Moreira JC (2013) Exploring the multifactorial nature of autism through computational systems biology: calcium and the Rho GTPase RAC1 under the spotlight. Neuromolecular Med 15:364–383.